Arch Virol (1993) 130: 269–277

Archives of Virology

Genetic restriction of murine hepatitis virus type 3 expression in liver and brain: comparative study in BALB/c and C3H mice by immunochemistry and hybridization in situ

D. Décimo[1, 2], Odile Boespflug[1], M. Meunier-Rotival[2], Michelle Hadchouel[2], and M. Tardieu[1]

[1] Laboratoire de Neurovirologie et de Neuroimmunologie, Université Paris XI and [2] INSERM Unité 347 affiliée au CNRS, Hôpital de Bicêtre, Le Kremlin-Bicêtre, France

Accepted December 15, 1992

Summary. To study the host-dependent genetic variations in murine hepatitis virus type 3 (MHV 3) induced diseases, we localized the sites of MHV 3 (Mill Hill strain) expression within liver and brain by immunohistochemistry or hybridization in situ. Two strains of mice were studied: BALB/c mice, which develop an acute and lethal hepatitis and C3H mice which develop a chronic brain infection. In BALB/c mice, viral RNA and antigens appeared during the first 24 h post infection (p.i.) in liver, whereas viral RNA was barely detectable in brain, up until death at day 3 p.i. In C3H mice, viral RNA and antigens were detected simultaneously in liver and brain only at day 2 p.i. In brain, the virus was detected in meningeal and ependymal cells and in perivascular cortical areas (days 5 and 7 p.i.). After day 49, the virus was no longer detected in brain parenchyma, but persisted in meningeal cells. Two host-dependent genetic differences in viral processing were observed in the liver: (1) the virus was first detected in Kupffer cells in BALB/c mice and mostly in hepatocytes in C3H mice; (2) in BALB/c mice, the 180 kDa S viral glycoprotein appeared more frequently cleaved in 90 kDa form than in C3H mice.

Introduction

The origin of genetic variations in clinical expression of viral diseases is of major biological importance but is far from being completely understood. Experimental diseases induced in mice by coronaviruses allow a convenient approach to study this question, since the induced pathologies depend upon the genetic origin of the infected mice [12, 20]. Thus, intraperitoneal injection of murine hepatitis virus type 3 (MHV 3) into adult mice results either in early death (at day 3 to 4 post infection, p.i.) due to hepatitis in the BALB/c strain,

an absence of patent disease in the A/Jax strain, or in the development of neurologic symptoms in the C3H strain [4, 16–18, 20]. In the latter strain, central nervous system (CNS) lesions are different from those induced by other coronaviruses and consist of ependymitis, meningitis, and vasculitis followed by hydrocephalus. They are related to a chronic infection since a low viral titer can be detected in brain for several weeks after infection [16, 18]. Genetic variations in MHV 3-induced diseases were initially linked to differences observed in vitro in the rate of viral replication in host cells [1, 9, 11, 19].

The aim of the present work was to localize in vivo the sites of MHV 3 expression within liver and brain in two different strains of mice that develop two different diseases after infection. Localization was made by immunohistochemistry or hybridization in situ, using a specific anti-MHV 3 serum or an RNA probe of the 3′ end of the MHV 3 genome [5], respectively.

Materials and methods

Virus

MHV 3 of the Mill Hill strain was plaque purified and isolated as previously described [17]. The virus used throughout this work was derived from a single isolate of plaque purification and was stored at − 80 °C.

Mice

Inbred C3H/He and BALB/c mouse strains were obtained from the Centre de sélection et d'élevage d'animaux de laboratoire, Orléans, France, or from Iffa-credo, France. The absence of circulating MHV 3 antibodies was verified by enzyme-linked immunosorbent assay (ELISA). Twelve to thirteen week old mice were infected by intraperitoneal injection of 1×10^2 PFU/animal. At different times after infection, the animals were killed by cervical dislocation and brain and liver were removed, frozen in isopentane in liquid nitrogen and stored at − 80 °C pending analysis. For each tested time, two to four different animals of each strain were analyzed.

Intratissular viral proteins

Frozen liver samples were homogenized in 250 mM sucrose, 1 mM ethylene glycol-bis(β amino-ethyl ether) tetraacetic acid (EGTA), 10 mM Tris-HCl pH 7.5, 0.1 mM phenylmethylsulfonyl fluoride. Plasma membranes and microsomes were prepared as previously described [3]. The quantity of liver proteins, analyzed on sodium dodecyl sulfate-polyacrylamide gel electrophoresis (SDS-PAGE) and immunoblotting, was adjusted so as to contain the same viral titer, evaluated in PFU [4, 17]. The titers of the virus in tissue of the different mouse strains on different days remained in the previously published range [4, 17]. Immunoblots were quantified by scanning densitometry.

Antibody

Polyclonal antibodies against MHV 3 were prepared by immunizing a rabbit with purified MHV 3 following the procedure of Sturman et al. [15]. The serum was adsorbed against uninfected liver and brain mouse tissues and tested both by ELISA and SDS-PAGE.

Immunohistochemistry

6 μm thick frozen tissue sections fixed in acetone were incubated in a 1 : 100 dilution of the rabbit anti-MHV 3 serum in a solution containing 25% porcine normal serum and 1% bovine serum albumin, overnight at 4 °C. The slides were washed in PBS and anti-MHV 3 antibodies binding to tissue sections were revealed by a rabbit peroxydase-anti-peroxydase system (DAKO) with 3-amino-9-ethylcarbazole as substrate. The slides were counterstained with hematoxylin.

Hybridization in situ

A fragment of the MHV 3 nucleocapsid-encoding gene (from 649 to 1600) which is described in the accompanying paper [5] was cloned in a vector containing two RNA transcription promoters, Sp 6 and T 7 (pGEM 7 ZF, Promega) [10] and used for hybridization in situ. The riboprobe was radiolabeled (Kit Boehringer Mannheim France, Meylan) with [^{35}S]UTP (Amersham France, Les Ulis) and the specific activity was 1×10^8 cpm/μg. 6 μm tissue sections were fixed for 15 min in 4% formaldehyde solution at 4 °C and stored in 70% ethanol for 3 to 6 days. Hybridization in situ was performed as previously described [6]. The tissue sections were dipped in NTB 2 (Kodak) nuclear track emulsion and exposed for 1–6 weeks. The slides were counterstained with hematoxylin.

Results

Genetic differences in virus spread and cellular permissiveness for virus, in liver

In BALB/c mice, there was no liver injury during the first 24 h p.i. although viral RNA was already detected in 1% of Kupffer cells of liver cells at 16 h p.i. and viral proteins at 24 h p.i. By day 2 p.i., liver lesions consisted of necrotic foci of 5 to 10 cells surrounded by polymorphonuclear cells. At this time point, viral RNA and antigens were detected in both Kupffer cells and hepatocytes. Hepatocytes containing viral antigens were usually found close to Kupffer cells containing viral antigens (Fig. 1 A). Cells containing viral RNA were more numerous than cells containing viral antigens (ratio 1.5/1). A viral antigen staining was also observed in the triangular shaped fat storing cells (Ito cells) between hepatocytes, as well as in vascular endothelial cells (Fig. 1 A). Thereafter, necrosis became confluent and areas of viral detection increased in size and at the time of death, 60 to 80% of cells, or remains of them, in the liver were positive for viral antigens whereas only 10 to 20% were still positive for RNA.

In C3H mice, necrotic foci remained smaller and 10 times less numerous than in BALB/c mice. Viral RNA and proteins were first detected between days 1 and 2 p.i. and were localized simultaneously in hepatocytes and Kupffer cells (Fig. 1 B). Hepatocytes containing viral antigens were more numerous than Kupffer cells containing viral antigens. During the next few days, the intensity of detection increased slowly, up to a maximum reached between days 4 and 7 p.i. when 20 to 40% of liver cells expressed either viral antigens or viral RNA. Endothelial cells containing viral antigens were very infrequent and no Ito cells were labeled. By day 11 p.i., the number of positive cells decreased and by day

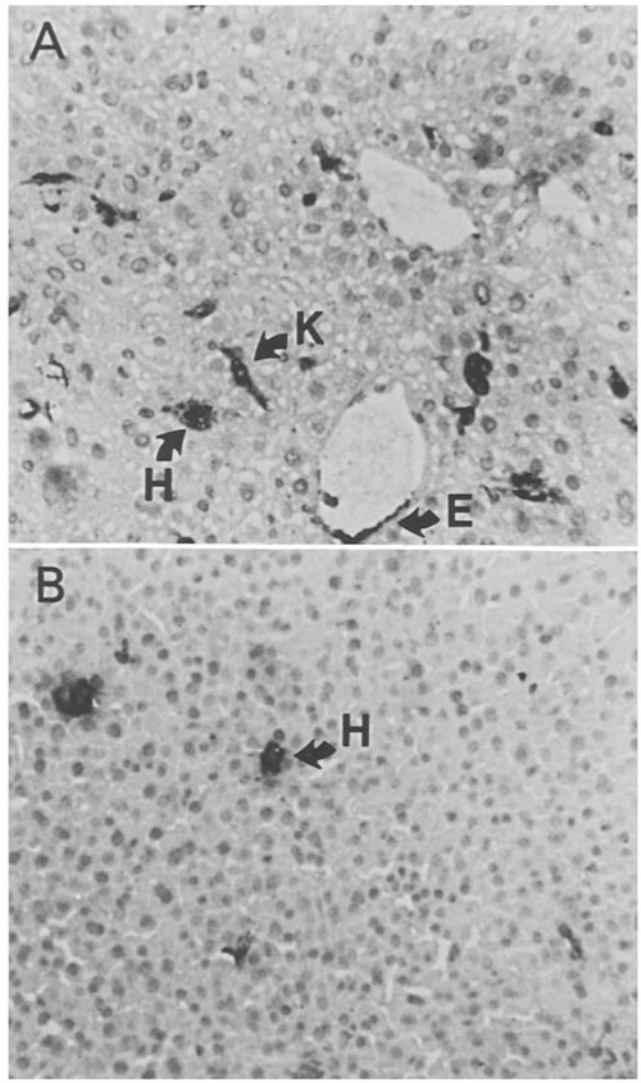

Fig. 1. Detection of MHV 3 antigens in BALB/c (**A**) and C3H (**B**) liver by immunohistochemistry. **A** and **B** Sections obtained at day 2 p.i. (× 75). *K* Kupffer cells, *H* hepatocytes, *E* endothelial cells. In BALB/c mice, Kupffer cells (which, at day 1, were the only antigen containing cells), hepatocytes and endothelial cells contain viral antigens, whereas in C3H mice viral antigen detection is mostly restricted to hepatocytes

21 p.i., RNA was no longer detected, whereas viral antigens were still found in a few cells. Liver morphology was normal at this time. From day 28 p.i., neither viral RNA nor antigens could be observed.

To analyze further genetic differences in the interaction between the virus and liver cells, viral structural proteins isolated from infected livers of both strains were compared by SDS-PAGE and immunoblotting. The amounts of liver proteins used in Western blots were adjusted so as to contain the same viral infectious titer (Fig. 2). Scanning densitometry shows a ratio of 2.5 between

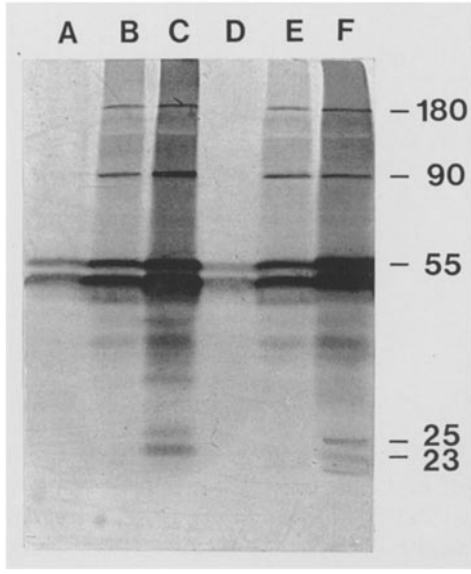

Fig. 2. Western blot analysis of intratissular viral proteins. *A–C* Proteins from BALB/c liver (*A* uninfected control liver, *B* liver obtained at day 2 p.i., *C* liver at day 3 p.i.). *D–F* Proteins from C3H liver (*D* control, *E* day 2 p.i., *F* day 4 p.i.). Amounts of proteins of liver membranes were adjusted so as to contain the same viral titer (*B* and *E* 10^4 PFU; *C* and *F* 10^6 PFU). The deduced masses of the reactive proteins are shown in kDa at the right

the 90 kDa S and the 180 kDa S bands in livers from BALB/c mice and of 1.5 in livers from C3H mice. In both strains, the unglycosylated 23 kDa protein was more abundant than the glycosylated 25 kDa protein. Finally, the bands at 51 and 55 kDa corresponding to the viral nucleocapsid N were identical in both strains.

Genetic differences in virus spread in brain

In BALB/c mice, neuropathological lesions consisted of a very low degree of meningeal infiltration in the mesencephalon ventral part, observed at day 3 p.i. just before the death of the animals. Viral RNA was found in meningeal cells only during the hours preceeding death (Fig. 3 A and B).

In C3H mice, viral RNA was first detected as early as day 2 p.i. and initially in the meninges, in ependymal cells of the III ventricle, around meningeal vessels, and in a few cells in areas of the cortex and diencephalon. At day 5 p.i., ependymal cells from lateral ventricles became positive (Fig. 4 B) as were widely separated areas in the cortex mostly around penetrating vessels, diencephalon and, less frequently, in the brain stem and the granular layer of the cerebellum. The abundance of viral RNA increased up to day 7 p.i. At that time, meningitis and ependymitis, the initial neuropathological lesions, could be first observed and viral RNA detection was widespread in ependymal cells and in the hypothalamus and thalamus, cortex, hippocampus, cerebellum, and brain stem (Figs. 4 C and 5 A–D). By day 11 p.i., signs of encephalitis and cortical vasculitis were present (Fig. 4 D) but viral RNA was less abundant. At day 15 p.i., ependymal cells of the lateral ventricles and aquaeduct as well as a few brain stem and cortical areas were still positive. At day 21 p.i., an intense meningeal vasculitis and a ventricular dilatation appeared which progressed up to day 77

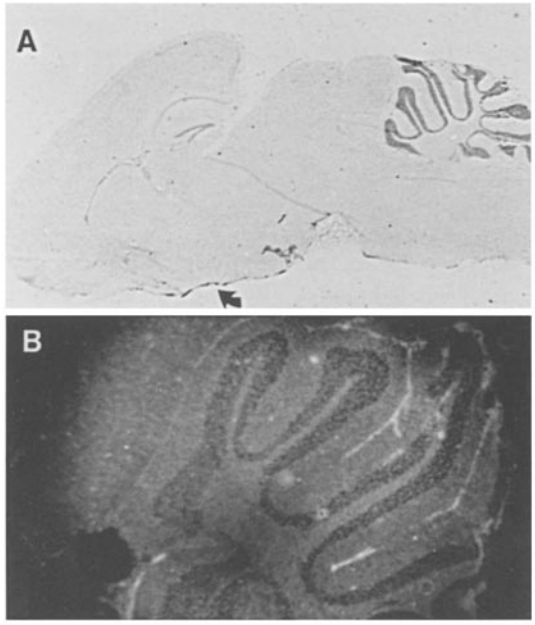

Fig. 3. Localization of viral RNA in brain of BALB/c mice by hybridization in situ at day 3 p.i. **A** Longitudinal section of whole brain (× 5); **B** cerebellum (dark field illumination) (× 75). Viral RNA is detected only in meningeal cells (arrow)

p.i., the last day tested (data not shown) [15]. Viral RNA could still be detected by day 49 p.i. in widely separated cortical areas and meningeal cells, and by day 77 p.i. in meningeal cells only. However, the intensity of the hybridization signal was low and required an exposure time of at least one month (Fig. 4 E and F).

Discussion

The spread of MHV 3 from the Mill Hill strain through the liver and to the brain and the permissiveness of the liver cells for the virus differed in BALB/c and C3H mice, two mouse strains that express two different clinical diseases after intraperitoneal infection by the virus. In BALB/c mice, viral RNA and antigens appeared early in liver but viral RNA was barely detectable in brain, up until the time of death at day 3 after infection. In contrast, in C3H mice, viral RNA and antigens were detected 24 h after infection simultaneously in liver and brain.

Several studies in vivo have failed to localize MHV 3 within the brain of C3H mice, although neuropathological lesions were dramatic [16, 18]. We previously observed in vitro that MHV 3 had a higher affinity for neurons, ependymal cells and meningeal cells than for astrocytes or oligodendrocytes [17]. The present study demonstrated this selective affinity of MHV 3 from the Mill Hill strain for these types of cells in vivo. It also gave an indication of the diffusion of the virus within the brain. Meningeal cells appeared to be the first infected cells. Thereafter, the virus was observed along the ependymal cell line and in increasingly larger perivascular cortical areas, finally disappearing from brain parenchyma, the last infected CNS cells being the meningeal cells. Thus,

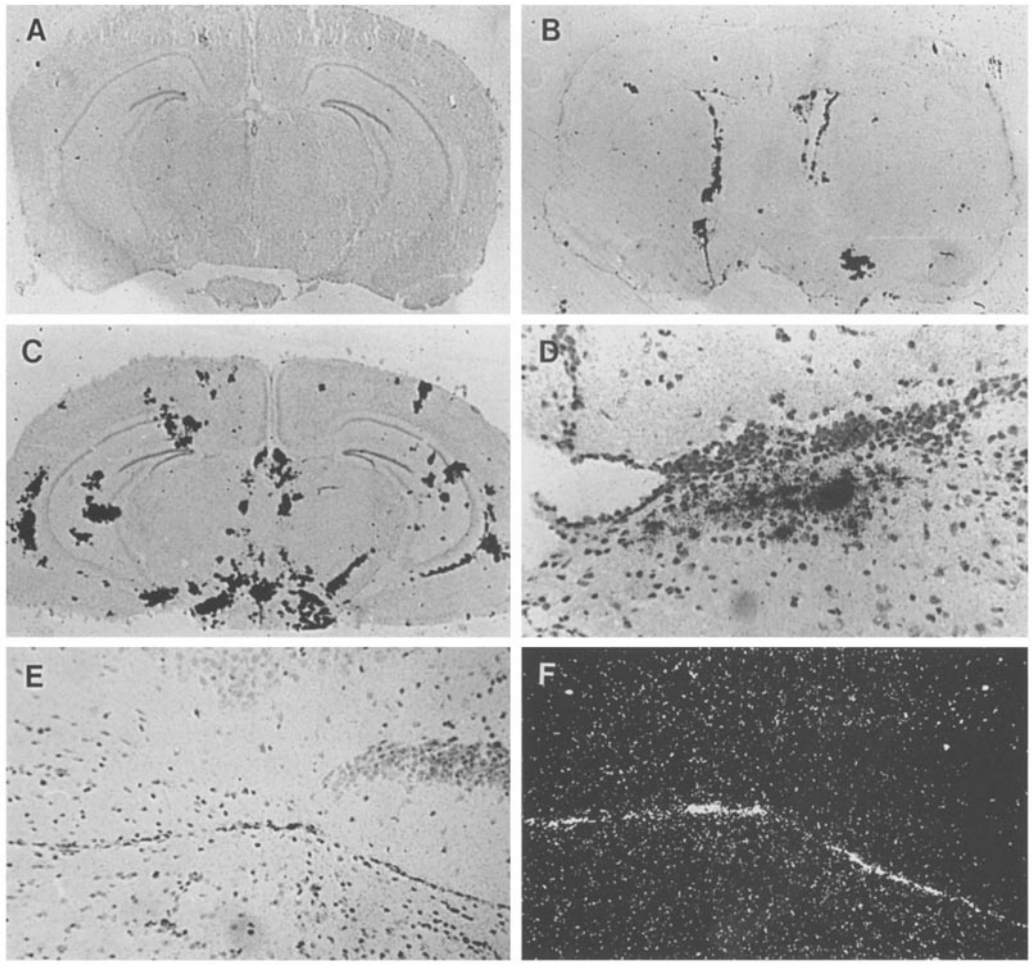

Fig. 4. Time sequence analysis of viral transcripts in C3H brain. Coronal sections of C3H brain, obtained at **B** days 5 (× 8), **C** 7 (× 8), **D** 11 (× 150), and **E**, **F** 77 p.i. (**E** bright field illumination; **F** dark field illumination; × 75) and **A** uninfected control section (× 8) were hybridized with MHV 3-specific [^{35}S]probe followed by hematoxylin staining. The first viral RNA containing cells appear to be ependymal cells (**B**) followed by cells in disseminated areas of cortex and diencephalon (**C** and **D**). After 77 days of infection, viral RNA detection was restricted to meningeal cells

MHV 3 from the Mill Hill strain differs from other coronaviruses in both its spread within brain and the type of cells it can infect [8, 13].

In C3H mice, the virus appeared to spread less rapidly through liver and earlier towards the brain than in BALB/c mice. This could be related to two host-dependent differences in early viral processing, as we observed. First, there is a genetic difference in MHV 3 affinity for Kupffer cells and hepatocytes between C3H and BALB/c mice, since the virus was first detected in Kupffer cells in BALB/c mice and mostly but not exclusively in hepatocytes in C3H mice. A similar genetic difference in viral affinity was observed with MHV JHM

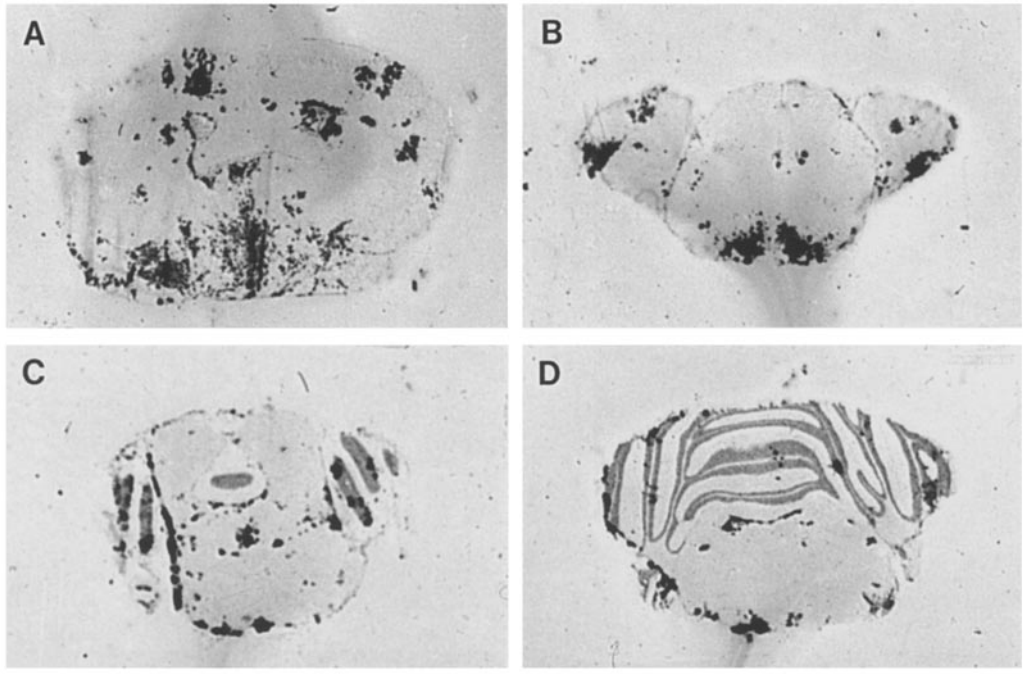

Fig. 5. Localization of viral RNA in different parts of the brain of C3H mice at day 7 p.i. Four representative coronal sections at the level of the lateral ventricles (**A**); diencephalon (**B**); rostal (**C**) and caudal (**D**) part of the IV ventricle and cerebellum. × 8

which was detected only in Kupffer cells in SJL mice but mostly in hepatocytes and in some Kupffer cells in BALB/c mice [2]. A second difference was the observation that the 180 kDa S viral glycoprotein appeared more frequently cleaved into 90 kDa S glycoproteins in the livers of BALB/c mice than in the livers of C3H mice. This could depend on a difference in cleavage ability of S proteins by Kupffer cells and hepatocytes, although a genetic control of intracellular transport or cleavage of S proteins could not be excluded. Such a difference in the ability of host cells to cleave the 180 kDa S glycoproteins of a coronavirus has already been demonstrated in vitro to be responsible for a higher cellular fusion activity induced by the virions [7, 14, 21]. One could hypothesize that Kupffer cells/macrophages, the first infected cells in BALB/c mice, may be more efficient for proteolytic cleavage of the S glycoprotein than hepatocytes, a situation that would induce a higher rate of cell fusions within the liver. A lower affinity of MHV 3 for Kupffer cells from the C3H lineage could allow larger amounts of virus to diffuse and invade the brain during the early stages of infection.

References

1. Arnheiter T, Baechi T, Haller O (1982) Adult mouse hepatocytes in primary monolayer culture express genetic resistance to mouse hepatitis virus 3. J Immunol 129: 1275–1281

2. Barthold SW, Smith AL (1984) Mouse hepatitis virus strains: related patterns of tissue tropism in suckling mice. Arch Virol 81: 103–112
3. Beaufay H, Amar-Costesec A (1976) Cell fractionation techniques. In: Korn ED (ed) Methods in membrane biology, vol 6. Plenum, New York, pp 1–100
4. Boespflug O, Godfraind C, Tardieu M (1989) Effect of cyclosporin A on a chronic viral CNS infection in mice. J Neuroimmunol 21: 49–57
5. Décimo D, Philippe H, Hadchouel M, Tardieu M, Meunier-Rotival M (1993) The gene encoding the nucleocapsid protein: sequence analysis in murine hepatitis virus type 3 and evolution in *Coronaviridae*. Arch Virol 130: 279–288
6. Etiemble J, Moroy T, Jacquemin E, Tiollais P, Buendia MA (1989) Fused transcripts of c-myc and a new cellular locus, hcr in a primary liver tumour. Oncogene 4: 51–57
7. Frana MF, Behnke JN, Sturman LS, Holmes KV (1985) Proteolytic cleavage of the E 2 glycoprotein of murine coronavirus: host dependent differences in proteolytic cleavage and cell fusion. J Virol 56: 912–920
8. Jordan CA, Friedrich VL, Godfraind C, Cardellechio CB, Holmes KV, Dubois-Dalcq M (1989) Expression of viral and myelin gene transcripts in a murine CNS demyelinating disease caused by a coronavirus. Glia 2: 318–329
9. Lamontagne LM, Dupuy JM (1984) Natural resistance of mice to mouse hepatitis virus type 3 infection is expressed in embryonic fibroblast cells. J Gen Virol 65: 1165–1170
10. Melton DA, Kreig PA, Rebagliati MR, Maniatis T, Zinn K, Green MR (1984) Efficient in vitro synthesis of biologically active RNA and RNA hybridization probes from plasmids containing a bacteriophage SP 6 promoter. Nucleic Acids Res 12: 7034–7059
11. Pereira CA, Steffan AM, Kirn A (1984) Interaction between mouse hepatitis virus and primary cultures of Kupffer and endothelial liver cells from resistant and susceptible inbred mouse strains. J Gen Virol 65: 35–44
12. Siddell S, Wege H, Ter Meulen V (1983) The biology of coronaviruses. J Gen Virol 64: 761–776
13. Sorensen O, Dales S (1985) In vivo and in vitro models of demyelinating disease: JHM virus in the rat central nervous system localized by in situ cDNA hybridization and immunofluorescent microscopy. J Virol 56: 434–438
14. Sturman LS, Ricard CS, Holmes KV (1985) Proteolytic cleavage of the E 2 glycoprotein of mouse coronavirus: activation of cell-fusing activity of virions by trypsin and separation of two different 90 K cleavage fragments. J Virol 56: 904–911
15. Sturman LS, Holmes KV, Behnke J (1980) Isolation of coronavirus envelope glycoproteins and interaction with viral nucleocapsid. J Virol 33: 449–462
16. Tardieu M, Goffinet A, Harmant van Rijckevorsel G, Lyon G (1982) Ependymitis, leukoencephalitis, hydrocephalus, and thrombotic vasculitis following chronic infection by mouse hepatitis virus 3 (MHV 3). Acta Neuropathol 58: 168–176
17. Tardieu M, Boespflug O, Barbé T (1986) Selective tropism of a neurotropic coronavirus for ependymal cells, neurons, and meningeal cells. J Virol 60: 574–582
18. Virelizier JL, Virelizier AM, Allison AC (1975) Neuropathological effects of persistent infection of the mice by mouse hepatitis virus. Infect Immunol 12: 1127–1140
19. Virelizier JL, Allison AC (1976) Correlation of persistent mouse hepatitis virus (MHV 3) infection with its effect on mouse macrophage cultures. Arch Virol 50: 279–285
20. Wege H, Siddell S, Ter Meulen V (1982) The biology and pathogenesis of coronaviruses. Curr Top Microbiol Immunol 99: 165–200
21. Yoshikura H, Tejima S (1981) Role of protease in mouse hepatitis virus-induced cell fusion. Virology 113: 503–511

Authors' address: M. Tardieu, Laboratoire de Neurovirologie et Neuroimmunologie, Université Paris XI, 80 rue du Général Leclerc, F-94276 Le Kremlin-Bicêtre Cedex, France.

Received July 21, 1992